

Adsorption of PEO in Highly Confining Porous Glass

H. Gr \ddot{u} ll,[†] R. Shaulitch, and R. Yerushalmi-Rozen*

The Reimund Stadler Minerva Center for Mesoscale Macromolecular Engineering and the Department of Chemical Engineering, Ben-Gurion-University of the Negev, Beer-Sheva, 84105, Israel

Received May 21, 2001; Revised Manuscript Received August 27, 2001

ABSTRACT: Adsorption of poly(ethylene oxide) within porous glass, from aqueous solutions, was investigated as a function of the polymer molecular weight, pore diameter, concentration, and time, using differential refractometry. The kinetics of the process was found to depend on the ratio of pore diameter to the correlation length in the polymer solutions. The adsorbed amount exhibited a dependence on pore diameter for the longer molecular weights, with an unexpected observation of a higher adsorption in smaller pores. This observation is explained by the interplay between geometry-dependent enthalpic gain due to adsorption and entropic loss due to confinement.

Introduction

The effect of confinement on flexible polymers was investigated thoroughly in the past decades: Theoretical modeling and experimental observations¹ suggested that when the confining length scale (layer thickness in thin films^{2,3} or pore diameter, d , in porous media^{4–6}) is comparable to or smaller than the radius of the free coils, R_g , it dominates the behavior and properties of the trapped chains. For example, a single chain in good solvent conditions (dilute solution regime and $R_g \sim d$), which is trapped in a pore,⁴ rearranges into an array of blobs of diameter d . As a result, the extension of the chain along the pore, R_p , scales with the pore diameter as $R_p \cong aN(a/d)^{2/3}$. The entropic penalty of chain squeezing in the pores leads to a lower concentration of the chains as compared to the bulk solution, with a partition coefficient $K = C_{\text{pore}}/C_{\text{bulk}} = \exp(R_g/d)^{3/5}$.^{4, 7–9}

As the concentration increases, the pores become filled with sequences of blobs of length R_p until the blobs begin to overlap. The overlap concentration inside the pores does not depend on the degree of polymerization, N , and scales with the pore diameter $C_p^* \cong N/d^2 R_p \cong a^{-3}(a/d_p)^{4/3}$.¹⁰ Above the overlap concentration, the polymers are characterized by the correlation length, which scales with the pore diameter $\xi = d(C_p^*/C)^{3/4}$. Here as well, d replaces R_g as the dominant length scale. When the bulk concentration exceeds C^* , a transition from weak to strong penetration, due to the bulk osmotic pressure, is observed. The partition coefficient becomes $K_{\text{conc}} = C_{\text{pore}}/C_{\text{bulk}}^* = K_{\text{dilute}} \exp(C_{\text{bulk}}/C_{\text{bulk}}^*)^{5/4}$.⁶

Pores, cavities, and capillaries are of vital interest in applications such as size exclusion chromatography,¹¹ catalysis, controlled drug release,¹² and membrane filtration.^{8,9} While theoretical models that describe these systems assume, for simplicity, nonadsorbing walls, in many cases the dissolved polymers adsorb to the inner walls of the media. Recent computer simulations considered the effect of adsorption on chromatographical separation of polymers and block polymers.¹³

Adsorption of flexible homopolymers at the solid–liquid interface is one of the oldest subjects investigated

by polymer science.^{14–16} Yet, only the effect of flow on adsorption within porous media has been described theoretically.¹⁷

We suggest that in the case of adsorbing walls a nonzero value of the segmental adsorption energy, ϵ , may lead to an overall gain in free energy that can compensate for the loss in entropy due to chain squeezing in the pore. Consequently, the polymer concentration within the pore is expected to be higher than in the case of a nonadsorbing wall. In this system, the total surface coverage Γ (polymer mass per surface area) may depend on the pore diameter d or on the ratio $r^* = d/R_g$ in addition to the dependence on the concentration and solvent quality: Confinement of the chains in the pores introduces an artificial cutoff length, thus limiting the maximal loops and tail size. In extreme cases, where $d \ll R_g$, the adsorbing chains may adopt a flat configuration, where all segments are in contact with the surface, leading to a value of Γ which is much lower than in the nonconfined case and dependent on pore diameter.

Studies of adsorption in porous materials are experimentally challenging: While many experimental studies investigated adsorption on flat surfaces,¹⁴ adsorption within porous media was investigated only in a few model systems^{18,19} such as capillaries under controlled-flow conditions.²⁰ In these studies, the measured hydrodynamic radius was used as a sensitive probe to the loop–tail–train distribution of the adsorbed layer. Yet, these methods cannot measure independently the absolute value of the adsorbed amount.

Here we report the use of a classical method, differential refractometry,²¹ for the measurement of the total surface coverage, Γ , of PEO adsorbed within controlled porous glass (CPG) from aqueous solutions. It is known that PEO monomers adsorb to glass via hydrogen bonding with the surface silanol groups. The adsorption is reversible and pH-dependent.²⁰ The glass is highly porous, with well-defined pore diameters of 8 and 89 nm. For the molecular weights investigated here, the corresponding values of r^* are in the range of $0.1 < r^* < 22$. Using a differential refractometer, the depletion of the adsorbed species from the bulk solution is measured directly with a characteristic sensitivity of $\delta y = \pm 1 \times 10^{-5}$ (y = mass fraction of PEO). In this method the observable is the difference in the PEO concentration in solution. Therefore, the calculation of the ad-

[†] Present address: Philips Research Laboratories, Prof. Holstlaan 4, 5656 AA Eindhoven, The Netherlands.

* To whom correspondence should be addressed. E-mail rachely@bgumail.bgu.ac.il.

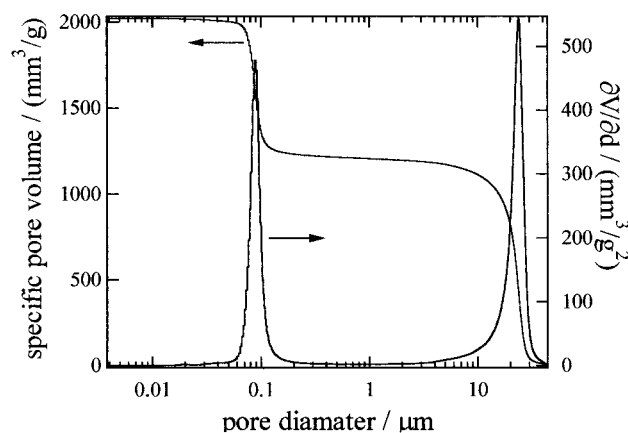


Figure 1. Pore size distribution of CPG89 measured with mercury porosimetry. The first peak corresponds to the average pore size ($d = 89 \pm 5$ nm), and the second peak results reflects the average particle size (30–60 μm) of the densely packed porous glass powder.

Table 1. Characteristics of PEO Samples

| polymer | M_w (g mol $^{-1}$) | M_w/M_n | N | R_g^a (nm) | c^*, b (g/cm 3) |
|---------|------------------------|-----------|-------|--------------|-----------------------|
| PEO9K | 9 202 | 1.07 | 209 | 4.02 | 0.0561 |
| PEO78K | 77 592 | 1.06 | 1763 | 13.8 | 0.0116 |
| PEO1.3M | 1 300 000 | 1.14 | 29545 | 71.0 | 0.0014 |

^a Calculated following the relation $R_g^{\text{exp}}/\text{nm} = 0.0202 M_w^{0.58 \cdot 23}$

^b Calculated using the experimental value of R_g^{23} . $C^* = 3M_w/(4\pi N_A R_g^3)$.

Table 2. Characteristics of the Controlled Pore Glass

| glass | d_{pore} (nm) | a° (m 2 /g) | specific pore vol, mL/g | particle size (μm) |
|-------|------------------------|-----------------------|-------------------------|---------------------------------|
| CPG8 | 7.7 | 182 | 0.47 | 38–75 |
| CPG89 | 89 | 34.2 | 0.90 | 30–60 |

sorbed amount is model-independent and is not affected by the exact conformation of the adsorbed layer or the detailed structure and interactions of the adsorbing substrate.

In the following we describe a series of experiments in which the adsorption of PEO from an aqueous solutions was determined as a function of polymer molecular weight, concentration, and pore size of the CPG. We investigate the kinetics of the adsorption process, and the overall adsorbed amount, and discuss the effect of confinement.

Experimental Section

Materials. Poly(ethylene oxide) (PEO) of different molecular weight M_w was purchased from Polymer Source, Canada, and Polymer Laboratories, UK (Table 1). Controlled pore glass (CPG) with a narrow pore distribution was obtained from Schott Gerte GmbH, Mainz, Germany, and Sigma-Aldrich (Table 2). The CPG89 was characterized by Porotec GmbH, D-65719 Hofheim, Germany, while the CPG8 was characterized by the manufacturer. The size distribution of the CPG89 is presented in Figure 1.

Sample Preparation. We used Millipore water (Milli-Q Plus system) to prepare all PEO/water solutions by weight. Solutions in a concentration range of $0 < y < 0.025$ [y = mass fraction of PEO, $y = m_{\text{PEO}}/(m_{\text{PEO}} + m_{\text{water}})$; $\delta y = \pm 1 \times 10^{-5}$] were investigated.

Great care was taken to purify the porous glass from water-soluble contaminants of relatively high refractive index (e.g., salts). First, the porous glass was boiled 2 h in a mixture (1:3 by volume) of HCl (28 wt %) and concentrated HNO $_3$ (30 wt %). After thorough washing with water, the glass was transferred into a Soxhlet apparatus and was continuously ex-

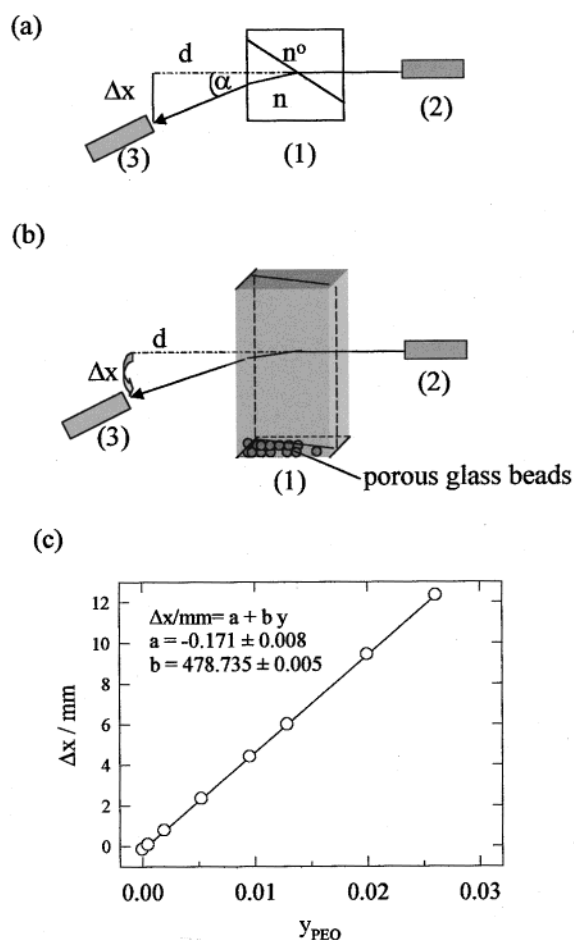


Figure 2. Differential refractometer.²² (a) A schematic representation of the optical system (1), the diagonally partitioned quartz glass cell (5 cm \times 2 cm \times 2 cm) (2), and the laser (He: Ne 10 mW) (3). The detection system includes an optical ruler and a bisected photodiode, $d = 186$ cm. (b) Side view showing glass beads (the porous glass) on the bottom of one compartment. The laser beam passes above the beads and through the liquid. (c) A typical calibration curve, presenting the measured Δx value as a function of the solution mass fraction, in PEO/water mixture.

tracted in water for 2 weeks. The glass was dried under vacuum (1 Torr) at $T = 150$ $^\circ\text{C}$, which is sufficient to overcome the capillary condensation of water trapped in the pores.

Technique. Adsorption measurements were carried out using a differential refractometer (DR) which measures the difference of refractive index between two liquids. The apparatus is described schematically in Figure 2. A laser beam passes through a rectangular quartz glass cell [Figure 2 (1)] which is diagonally partitioned into two compartments. The compartments contain two liquids of different refractive index. In our experiments one of the compartments is filled with water (refractive index n^0) and serves as a reference liquid for the second compartment which is filled with PEO/water solution (of a refractive index n). The cell is tightly sealed with Teflon stoppers to prevent evaporation. As the incident laser beam (2) passes through the cell, it is deflected by an angle, α , proportional to the difference in the refractive index $\Delta n = n^0 - n$, between the water and the PEO/water solution (Snell law). A detection system (3) measures the deflection of the beam, Δx , at a distance of $d = 186$ cm from the incidence point, where Δx is proportional to Δn . The large distance is the origin of the high resolution of the apparatus with $\delta \Delta n = \pm 5 \times 10^{-5}$. In the experimental concentration range, the refractive index of the PEO/water solution is linearly proportional to the mass fraction of PEO. The deflection of the laser beam Δx is calibrated using PEO/water solutions of known mass fraction. A typical calibration curve is presented in Figure 2c. The

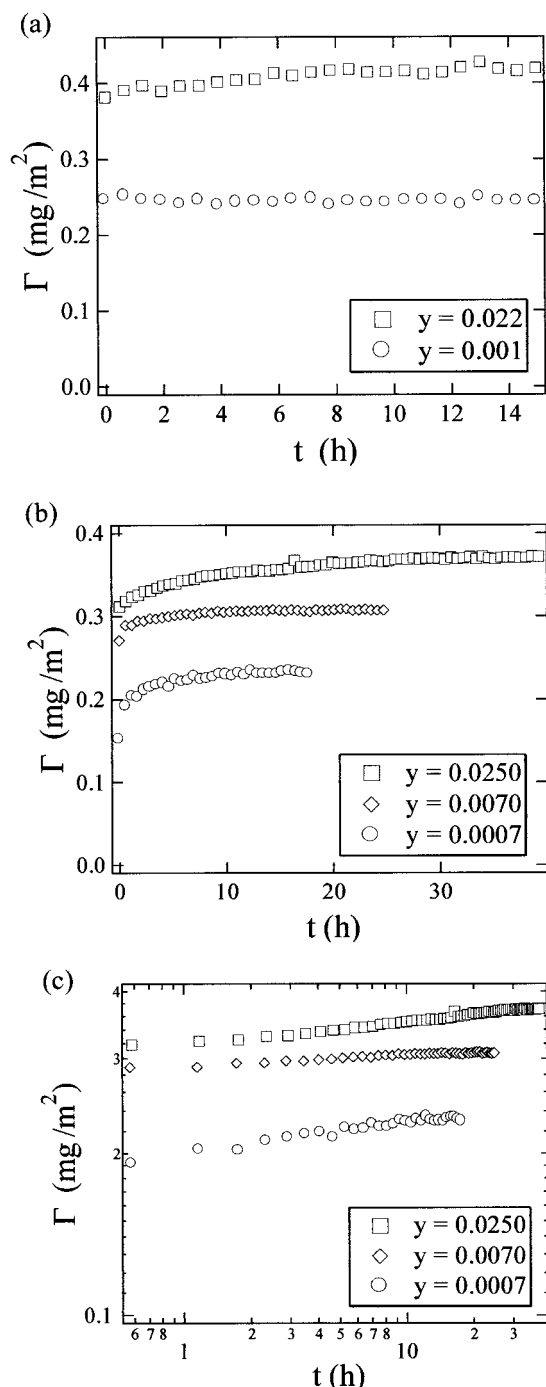


Figure 3. Total surface coverage Γ (mg/m^2) of PEO9K within CPG89 as a function of time. (a) Two different initial concentrations: (\square) $y = 0.022$ and (\circ) $y = 0.001$. (b) Adsorption within CPG8 at three different initial concentrations: (\square) $y = 0.0250$, (\diamond) $y = 0.0070$, and (\circ) $y = 0.0007$. (c) A double-logarithmic plot of (b).

resulting precision of the apparatus in determining the mass fraction of PEO, δy , is $\delta y = \pm 1 \times 10^{-5}$. In these experiments, a high thermal stability is required, as the refractive index is temperature-dependent. In the present setup, temperatures fluctuations, δT , are of the order $\delta T = \pm 1$ mK. All the adsorption measurements described in this study were carried at a constant temperature of $T = 25 \pm ^\circ\text{C}$ and pH of 6.2.

Adsorption Measurements. In a typical experiment, a known mass m^0 of a PEO/water mixture is filled into one compartment of the cell (Figure 2) and the initial concentration y^0 is measured. Next, a known mass of porous glass, m_{glass} , is added to the mixture and vigorously stirred. During the measurement, stirring is repeated every 10 min. After stirring,

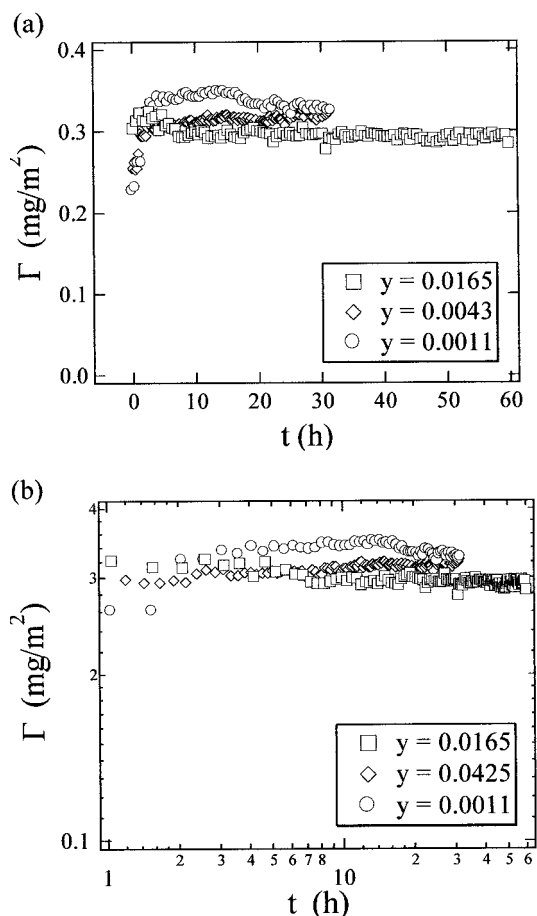


Figure 4. Total surface coverage Γ (mg/m^2) of PEO1.3M within CPG89 as a function of time at three different initial concentrations: (\square) $y = 0.0165$, (\diamond) $y = 0.0043$, and (\circ) $y = 0.0011$. (a) A linear plot; (b) a double-logarithmic plot.

the porous glass is allowed to settle down, and the laser beam passes through the liquid above it (Figure 2b). The adsorption of PEO within the CPG causes a depletion of PEO from the bulk solution (above the glass) and therefore changes the mass fraction y of the solution. The adsorbed amount of PEO is calculated using eq 1.

$$\Gamma_{\text{PEO}} = \frac{m^0}{m_{\text{glass}} - a^0}(y^0 - y) \quad (1)$$

m^0 is the mass of PEO/water mixture, m_{glass} the mass of CPG, and a^0 the specific surface area of the CPG. Typical values are $m^0 \sim 1.69$ g, $m_{\text{glass}} \sim 0.048$ g, $a^0 \sim 34$ m^2/g , $y^0 = 0.0148$, and $y^{\text{eq}} = 0.0144$.

Results

In this study we investigated the adsorption of PEO from aqueous solutions within porous glass of two different pore diameters [$d = 8$ nm (CPG8) and 89 nm (CPG89)] as a function of concentration polymer molecular weight and time.

In Figure 3 we present the time dependence of the adsorption of PEO9K within CPG89 (a) and CPG8 (b,c). We observe that while in the big pores (Figure 3a, $r^* \sim 23$) the adsorption takes place almost instantaneously, adsorption in the small pores (Figure 3b, $r^* \sim 2$) is considerably slower. Up to 20 h is required to reach the final value of Γ (Figure 3b,c). A weak dependence of the kinetics on the initial concentration is observed.

Figure 4 presents the adsorption kinetics of PEO1.3M in CPG89 ($r^* = 1.3$) at different initial concentrations

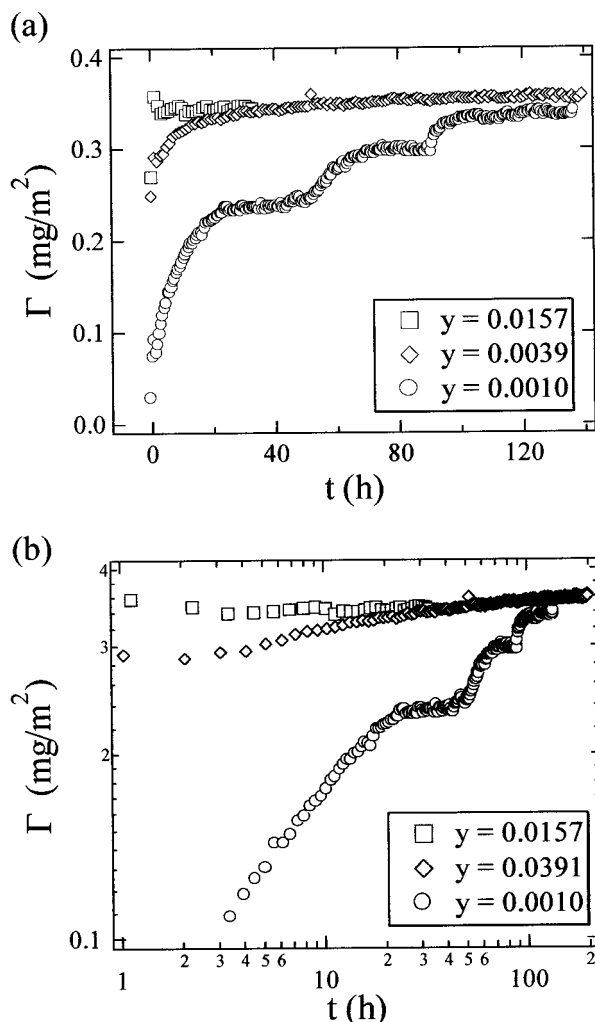


Figure 5. Total surface coverage Γ (mg/m^2) of PEO1.3M within CPG8 as a function of time at three different initial concentrations: (\square) $y = 0.0157$, (\diamond) $y = 0.0039$, and (\circ) $y = 0.0010$. (a) A linear plot; (b) a double-logarithmic plot.

in a linear (a) and a double-logarithmic plot (b). At this pore size the adsorption is fast, and the rate is independent of the initial concentration. The final value of Γ is reached within 5 h. A very different behavior is observed in Figure 5, where the time dependence of the adsorption of 1.3M PEO within CPG8 is presented ($r^* = 0.1$). We observe a strong dependence of the adsorption rate on the initial concentration. For the lowest concentration, $y = 0.001$, multiple plateaus (Γ vs time) at intermediate times are observed. The final value of Γ is attained after about 5 days (Figure 5a). In Figure 5b the adsorption kinetics is presented in a double-logarithmic plot. The linear part indicates that the different adsorption steps are diffusion-limited and are characterized by different diffusion constants. With increasing initial concentration the adsorption kinetics becomes faster and is almost instantaneous for the highest concentration $y = 0.016$, though this solution is very viscous. In Figure 6 we present adsorption isotherms (Γ vs y) for three different molecular weights in CPG89 (Figure 6a) and CPG8 (Figure 6b). For both adsorbents the low molecular weight PEO9K exhibits a low affinity adsorption isotherm and reaches a plateau value at fairly low concentrations ($y > 0.015$). This plateau value is slightly higher for the bigger pore size CPG89 as compared to the smaller pore size, CPG8. A

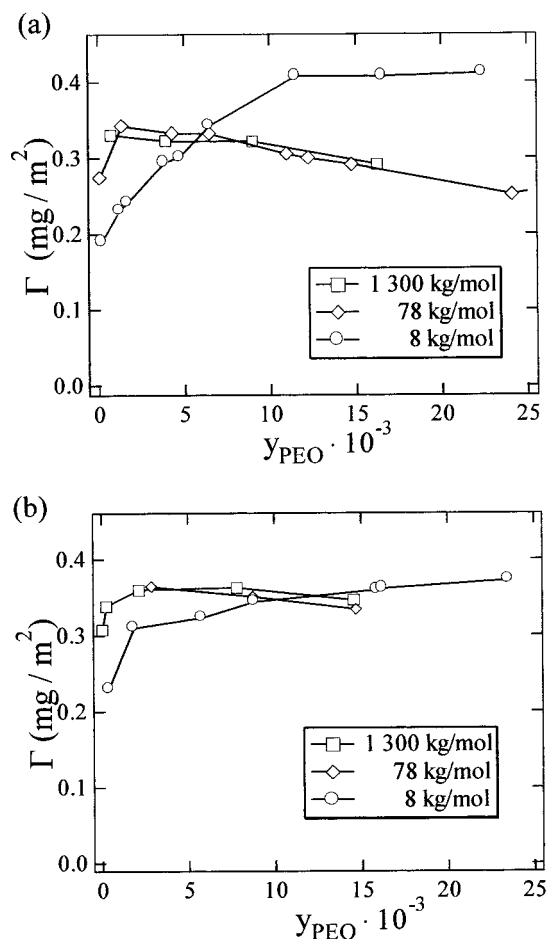


Figure 6. Adsorbed amount of PEO with various molecular weights as a function of steady-state concentration on (a) CPG89 and (b) CPG8.

different behavior is observed for PEO78K and PEO1.3M: The adsorption isotherms pass through a maximum value in a concentration range of $0.002 < y < 0.008$ and decline with further increase in the bulk concentration. At the high concentration regime, we observe that the plateau value of the isotherm Γ^∞ is smaller for both PEO78K and PEO1.3M than that of PEO9K. This observation is valid for both CPG8 and CPG89. An unexpected observation is that the adsorption, Γ^∞ , of PEO78K and PEO1.3M is higher within CPG8 than within the bigger pores of CPG89.

Discussion

In this study we used differential refractometry to investigate the kinetic and steady-state behavior of aqueous solutions of PEO in the presence of controlled porous glass (CPG).

We found that while PEO9K and PEO78K adsorbed instantaneously at all measured concentrations, on both CPG8 and CPG89, the adsorption rate of PEO1.3M exhibited a dependence on the pore diameter and the initial concentration of the solution. Adsorption of PEO 1.3M on CPG89 was fast, comparable to that of the lower molecular weight polymers, especially when the higher viscosity of the solution is taken into account. A very different behavior was observed in the case of CPG8. Here we found a strong dependence on the initial concentration of the solution. In particular, at the low concentration regime we observed a multiple plateau behavior, a single slope at intermediate concentrations,

and an instantaneous adsorption at high concentrations. The dependence on the initial concentration results from the dependence of the relevant diffusion coefficient on the correlation length: in the dilute regime the diffusion coefficient is given by²³

$$D = \frac{k_b T}{6\pi\eta R_H} \quad (2)$$

where k_b is the Boltzmann constant, T is the absolute temperature, η is the solvent viscosity, and R_H is the hydrodynamic radius of the polymer. In the semidilute regime, the chains overlap and the correlation length ξ is smaller than the coil radius and decreases further with increasing concentration. The relevant diffusion coefficient becomes then D_{conc} .⁶

$$D_{\text{conc}} = (1 - \phi)Dc = (1 - \phi)\frac{kT}{6\pi\eta\xi} \quad (3)$$

where $\phi = Ca^3$. It is known that transport in a semidilute solution is as much as 2 orders of magnitude faster than in dilute solutions.¹⁰ Both the small correlation length and the higher osmotic pressure in more concentrated solutions (above c^*) of PEO1.3M facilitate a more rapid penetration into the CPG8 and therefore a faster equilibration.

The multiple-plateau behavior observed at the low concentration regime ($C < C^*$) reflects a typical single-chain behavior: To penetrate into the pore, a chain has to unfold. The plateau regions in the graph reflect the time span, where many single chains unfold and slowly penetrate into the pores while effectively blocking the access to the pores for other polymer molecules. This behavior is modified at concentrations above C^* , where interchain entanglements lead to the formation of a transient network with a mesh size ξ , the relevant length scale in this regime. The higher osmotic pressure at $C > C^*$ results in a much higher penetration, resulting in the observed kinetics.

We observe that the adsorption isotherms of the high molecular weight polymers exhibit a high affinity behavior, similar to the behavior in nonconfining environment. The low molecular weight PEO9K deviates from this behavior, in agreement with previous observations.¹⁴ An unexpected feature of the adsorption isotherms of the higher molecular weight polymers (PEO78K, PEO1.3M) is a local maximum.

To discriminate between a kinetic and a thermodynamic origin of the observed maximum, we performed the following adsorption experiment: CPG89 was incubated in PEO78K at an initial concentration corresponding to $y = 0.026$ (a high concentration regime, denoted by H). Following the usual experimental protocol, the system was allowed to reach a steady state and the value Γ_H was noted. Then, the solution was diluted to a concentration $y = 0.008$ (a low concentration regime, denoted by L). This concentration corresponds to the concentration where the maximum of Γ was observed (Figure 6a). The system was allowed to reach a steady state, and the new value of Γ_L was measured. We found that $\Gamma_L > \Gamma_H$. This suggests that the maximum is not of a kinetic origin but rather represents a steady-state behavior. A similar observation of a maximum in the adsorption isotherm was reported by Eletkova et al.²³ for poly(ethylene glycol) in water, yet the origin of the phenomenon was not discussed. We suggest that the observed maximum may originate from a conformational transition triggered by the concentra-

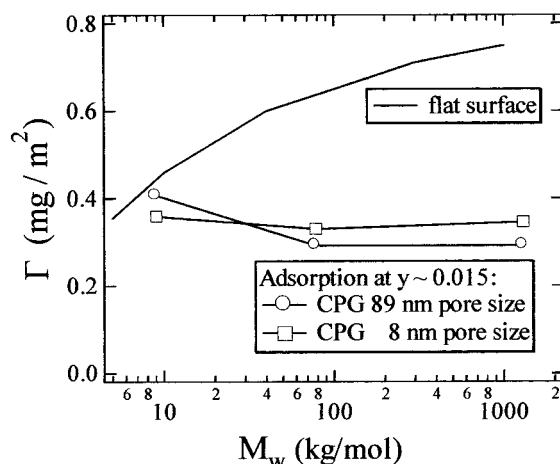


Figure 7. Steady-state value of the adsorbed amount of PEO at a concentration $y = 0.015$, Γ^∞ , in CPG89 (○) and CPG8 (□) and experimental data for a flat surface.²⁵

tion of the solution. As the observable in DR experiments is the total adsorbed amount, we are not able to test this assumption at this stage of the study.

In general, the question of whether the value of Γ measured in our experiments corresponds to thermal equilibrium or to a steady state is relevant to the interpretation of the data. It is known that relaxation processes of adsorbed chains are slow, and are even more so in porous media, at high solution concentrations. It is therefore reasonable to assume that the initially adsorbed layer is in a state of incomplete equilibrium that reflects the history of the system. Relaxation to a steady state (or preferably thermal equilibrium) might continue for a few weeks. From the experimental point of view, this requires long-term monitoring of Γ in a well-controlled environment. In particular, a high long-term thermal stability is required. Indeed, in this study the temperature fluctuations, δT , were of the order $\delta T = \pm 1$ mK over weeks, and that allowed us to monitor the value of Γ over weeks. We believe that the reported values represent a long-lived steady state, if not complete thermal equilibrium.

The most noteworthy observations of this study are summarized in Figure 7: We present the plateau values of the surface coverage Γ^∞ for CPG89 and CPG8 along with a experimental data of Γ^∞ taken from ref 25. The first observation relates to the measured value of Γ^∞ for the different molecular weights: Unlike the case of flat surfaces, we find that $\Gamma^\infty_{\text{PEO9K}}$, the adsorption of the lowest molecular weight polymer PEO9K, is higher than that of the higher molecular weight polymers. In addition, the value of $\Gamma^\infty_{\text{PEO9K}}$ in CPG89 is higher than that in CPG8. We suggest that both observations are a manifestation of the degree of confinement experienced by the polymer: PEO9K is less confined by both CPG's than the higher MW polymers and is effectively nonconfined in the 89 nm pores of CPG89. For the two polymers of the higher molecular weights, we find that the relevant length scale that determines the adsorbed amount is the pore diameter. This is conceptually different from observations of polymer adsorption in a nonconfining media, where a molecular weight dependence is expected. We note that it is the pore diameter, d , rather than the ratio r^* that determines the value of Γ . This observation may be explained by realizing that in a confined media the adsorbed amount is mainly determined by the number of monomers in contact with

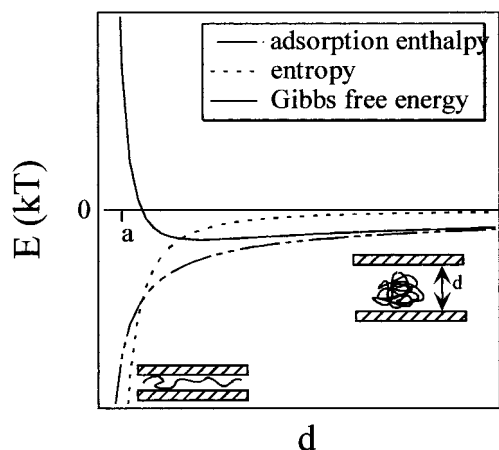


Figure 8. Dependence of the entropy, enthalpy, and Gibbs free energy of polymeric chains on pore diameter in a case of adsorbing walls. The model assumes that the chains are not distorted by the attraction of the walls.

the wall that adsorb in a “train” configuration. In our system, this value is approximately 0.4 mg/m^2 .^{14,25} The second observation, which at first sight seems counter-intuitive, is that for the two longer polymers a higher value of Γ^∞ is measured for the smaller pore diameter (CPG8). One may expect a higher adsorption in the larger pores, i.e., CPG89. However, we suggest that the observed higher value of Γ^∞ for CPG8 may be explained by the following picture: When a polymer chain is confined in a tube of a diameter d , it suffers from entropy loss due to confinement. The entropy of the confined chain scales with the pore size²⁶ as $S \sim -N(a/d)^{5/3}$. In the case of an adsorbing wall, an enthalpy term has to be added to the consideration. The enthalpic gain, ΔH , is the segmental sticking energy, ϵ , multiplied by the number of contacts with the wall. To a first approximation, we may estimate ΔH by considering only the monomers that are forced into contact with the wall, due to squeezing of the chain into the pore. Under this assumption, the number of wall-segment contacts depends on the number of blobs²⁶ $b = N(a/d)^{5/3}$ multiplied by the contour length of a blobs (πd). The total enthalpy gain due to adsorption for a confined chain should scale with the tube diameter as $\Delta H = -\epsilon \pi d N(a/d)^{5/3}$. We can see that in this picture the enthalpic gain due to adsorption depends on d and increases with decreasing pore diameter. The idea that substrate geometry may affect the value of the adsorbed amount was recently discussed for a different geometry.²⁷ In Figure 8 we present a schematic description of the dependence of the enthalpic gain and entropic loss on pore diameter. Superposition of these two relations defines a regime in which decreasing pore diameter results in a net gain of the Gibbs free energy due to adsorption leading to a local minimum. Thus, we expect that for a given chain length, in a certain range of pore diameters, a higher adsorbed amount will be obtained for smaller pores. The exact location of the crossover between the regime in which the enthalpic gain dominates the adsorption, to the regime in which the entropic loss takes over, depends on the values of the prefactors and especially on the value of ϵ . For high values of ϵ the transition would occur at lower d values. Note that, as expected for an infinite value of d (flat surface), a positive value of ϵ will always lead to adsorption. We may now add an additional entropic loss due to adsorption-induced distortion, which may be as high as the difference between the enthalpic gain and the first-

approximation loss of entropy.

To summarize, we investigated the adsorption of PEO from aqueous solutions within porous glass (CPG) as a function of time, pore diameter, molecular weight, and concentration. We found that the adsorption rate is diffusion-controlled and depends on the ratio of pore diameter to the correlation length of the polymeric solution. For the long chain polymers, similar values of adsorption were measured for a given pore diameter. In addition, we identified a regime in which enthalpic interactions dominate over the loss of entropy due to confinement, leading to a higher adsorbed amount in narrower pores.

Acknowledgment. We thank Dietrich Woermann for his generosity and guidance, Jürgen Jopp for his help with some of the measurements, and Avi Halperin and Igal Szleifer for enlightening discussions. R.Y.-R. gratefully acknowledges The Joseph and May Winston Foundation Career Development Chair in Chemical Engineering and H.G. The Ilse Katz Center for Meso and Nano-Scale Science and Technology for their support.

References and Notes

- (1) Granick, S. In *Polymers in Confined Environment*; Springer-Verlag: Berlin, 1999.
- (2) Jones, R.; Kumar, S. K.; Hot, D. L.; Briber, R. M.; Russell, T. *Nature* **1999**, *149*, 400.
- (3) Reiter, G. *Phys. Rev. Lett.* **1992**, *68*, 75.
- (4) Daoud, M.; de Gennes, P. G. *J. Phys. (Paris)* **1977**, *85*, 35.
- (5) Brochard Wyart, F.; Raphael, E. *Macromolecules* **1990**, *23*, 2276.
- (6) Guillet, G.; Leger, L.; Rondelez, F. *Macromolecules* **1985**, *18*, 2531.
- (7) Brochard, F.; de Gennes, P. G. *J. Chem. Phys.* **1977**, *67*, 52.
- (8) Cassada, E. F. *J. Polym. Sci., Part B* **1967**, *5*, 773.
- (9) Cassada, E. F.; Tagami, Y. *Macromolecules* **1969**, *2*, 14.
- (10) Teraoka, I.; Langley, K. H.; Karasz, F. E. *Macromolecules* **1993**, *26*, 287.
- (11) Giddings, J. C. *Unified Separation Science*; John Wiley: New York, 1991.
- (12) Shalaby, W. *Polymers of Biological and Biomedical Significance*; American Chemical Society: Washington, DC, 1994.
- (13) Guttman, C. M.; Di Marzio, E. A.; Douglas, J. F. *Macromolecules* **1996**, *29*, 5723.
- (14) Fleer, G. J.; Cohen Stuart, M. A.; Scheutjens, J. M. H. M.; Cosgrove, T. *Polymers at Interfaces*; Chapman and Hall: London, 1993.
- (15) Pandey, R. B.; Milchev, A.; Binder, K. *Macromolecules* **1997**, *30*, 1194.
- (16) Aubouy, M.; Guiselin, O.; Raphael, E. *Macromolecules* **1996**, *29*, 7261.
- (17) de Gennes, P. G. *C. R. Acad. Sci. Paris* **1995**, *320*, 85.
- (18) Satterfield, C. N.; Colton, C. K.; Turckheim, B. D.; Copeland, T. M. *AIChE J.* **1978**, *24*, 937.
- (19) Buttersack, C.; Rudolph, H.; Mahrholz, J.; Buchholz, K. *Langmuir* **1996**, *12*, 3101.
- (20) Stuart, M. A. C.; Tamai, H. *Langmuir* **1988**, *4*, 1184.
- (21) Gröll, H.; Woermann, D. *J. Phys. Chem.* **1996**, *100*, 1105.
- (22) Gröll, H. Ph.D. Thesis, Cologne, Germany, 1996.
- (23) Strobl, G. *The Physics of Polymers*, 2nd ed.; Springer: Berlin, 1997.
- (24) Eltekova, N. A.; Eltekov, Y. A. Characteristics of Pore Structure of Adsorbents by Macromolecules Adsorption. *Proc. IVth. Int. Conf. Fundamentals of Adsorption*, 1992, Kyoto.
- (25) Dijt, J. C.; Stuart, M. A. C.; Hofman, J. E.; Fleer, G. J. *Colloids Surf.* **1990**, *51*, 141.
- (26) de Gennes, P. G. *Scaling Concepts in Polymer Physics*; Cornell University Press: Ithaca, NY, 1985.
- (27) Aubouy, M.; Raphael, E. *Macromolecules* **1998**, *31*, 4357.